Cross sections of laser-induced collisional processes: Excitation transfer and charge transfer

Sydney Geltman
Joint Institute for Laboratory Astrophysics, National Bureau of Standards and University of Colorado, Boulder, Colorado 80309-0440
(Received 8 December 1986)

The standard theory for laser- (or light-) induced collisional processes is applied to excitation transfer and charge transfer. Detailed calculations are carried out for specific processes which have been studied experimentally, with good understanding resulting for most of the observed features. We study the variation in cross-section magnitude and line shape with transfer laser intensity, and find characteristic differences between the excitation-transfer and charge-transfer processes.

I. INTRODUCTION

A laser-induced collisional process

$$A(i)+B(i)+\hbar\omega\rightarrow A(f)+B(f)$$

is one which requires *both* the absorption (or stimulated emission) of radiation and the presence of the atom-atom interaction for its completion, with state changes taking place in both of the participating atoms. Thus it differs from a simple line-broadening process

$$A(i)+B(i)+\hbar\omega\rightarrow A(f)+B(i)\ ,$$

where the absorption of radiation takes place in only one of the atoms, while the role of the other atom is simply to perturb the energy levels of the absorbing atom during a collision.

The first theoretical discussions of these processes for excitation transfer were by Gudzenko and Yakovlenko.[1] A complete description of them from the pseudomolecular point of view was given by Gallagher and Holstein.[2] Contributions to the theory from other points of view have been presented by a number of other authors.[3] Several review papers[4] have covered laser-induced collisional excitation transfer (LICET) and other laser-induced collision processes. At low laser intensities it is essential to treat the problem from a molecular (or perturbed-atom) point of view since the atom-atom forces are much larger than the laser-atom interactions. This leads to the characteristic asymmetric line shapes for LICET. As shown by Payne, Anderson, and Turner,[5] when the laser intensity is increased such that the transition probabilities become saturated the line shape tends to become symmetric.

Most of the many experimental observations of LICET processes have been made by the Harris,[6] and Cahuzac and Toschek[7] groups. They are qualitatively well understood in terms of the existing theory and the known van der Waals interactions. On the other hand, the process of laser-induced collisional charge transfer (LICCT)

$$A^+(i)+B(i)+\hbar\omega\rightarrow A(f)+B^+(f)$$

has only been observed in the laboratory by Wright *et al.*[8] Furthermore, it is characterized by relatively narrow profiles having large shifts from the asymptotic energy differences, which are not present in the LICET process and which have not been well understood in terms of earlier theoretical work on LICCT.[9]

Our objective in the present paper is to outline the general theory and apply it in detail to two cases which have been studied experimentally, namely the LICET process

$$\mathrm{Sr}(5p\ ^1P_1)+\mathrm{Li}(2s\ ^2S_{1/2})+\hbar\omega\rightarrow\mathrm{Sr}(5s^2\ ^1S_0)+\mathrm{Li}(4d\ ^2D_{5/2})\ ,$$

and the LICCT process

$$\mathrm{Ca}^+(4s\ ^2S_{1/2})+\mathrm{Sr}(5s^2\ ^1S_0)+\hbar\omega\rightarrow\mathrm{Ca}(4s^2\ ^1S_0)+\mathrm{Sr}^+(5p\ ^2P_J)\ .$$

We will identify the particular features of the two processes which lead to qualitatively different cross-section frequency shifts and shapes. The intensity dependence of the magnitude of the cross section and its profile will be studied.

II. BACKGROUND THEORY

The essential physical picture which allows a tractable evaluation of laser-induced collision cross sections is the semiclassical one of straight-line trajectories for the relative motion of the two atoms and a quantum evaluation of transition probabilities. A first-order expression for the transition amplitude in this picture is

$$a_{\mathrm{if}}(t)=-i\int d\mathbf{r}\,\psi_f^{(0)}(\mathbf{r},t)\int_{-\infty}^{t}dt'\int d\mathbf{r}'G(\mathbf{r},t;\mathbf{r}',t')V(\mathbf{r}',t')\times\psi_i^{(0)}(\mathbf{r}',t')\ , \tag{1}$$

where $\psi_{i,f}^{(0)}$ are eigenfunctions of $H-V$, V is an interaction, and G is the Green's function corresponding to $H-V$ (H is the full quantum Hamiltonian on the straight-line classical path). If V is taken to be H_r (the interaction of the atoms with the laser field) plus H_c (the interatomic interaction), then $G=G_a$ is a Green's function constructed of products of free-atom wave functions.

For lower laser intensities, such that $H_c\gg H_r$, a perturbative reduction of (1) should involve orders higher

 ©1987 The American Physical Society

than the first for H_c while keeping H_r to first order. As this would become a rather intractable calculation, one is led to the alternate treatment of (1) in which V is taken to be H_r alone. This requires that H_c now be included in $H-V$ and that $G=G_m$ is a quasimolecular Green's function. Using this representation, the first-order perturbation transition amplitude in the rotating-wave approximation as a result of a single collision becomes

$$|a_{if}| = \frac{E_0}{2}\left|\int_{-\infty}^{\infty} dt \exp\left[-i\int_0^t dt'\{\omega-[E_f(R')-E_i(R')]\}\right]\int d\mathbf{r}\,\Phi_f^*(\mathbf{r},\mathbf{R})\hat{\epsilon}\cdot\mathbf{r}\Phi_i(\mathbf{r},\mathbf{R})\right| , \quad (2)$$

where E_0 is the laser electric field magnitude and $\hat{\epsilon}$ is its direction of linear polarization. (We use atomic units throughout unless otherwise specified.) If the laser frequency is resonant with a transition in one of the initial-state atoms such that a Stark shift is present which would alter the value of $E_f(\infty)-E_i(\infty)$, then this shift, BE_0^2, should also be included in the phase factor above.

The transition cross section as a function of the laser detuning from the asymptotic energy difference,

$$\delta=\omega-[E_f(\infty)-E_i(\infty)] ,$$

is then

$$\sigma(\delta)=2\pi\int_0^{\infty} d\rho\,\rho P(\rho) , \quad (3)$$

where the transition probability $P(\rho)=|a_{if}|^2$. P and σ are also dependent on v through the classical trajectory assumed for $\mathbf{R}(t)$. Thus $\sigma(\delta)$ is the collisional cross section in the presence of a laser field and it also represents the absorption line shape for the laser-induced process that we are studying.

We will need to examine the adiabatic energies $E_i(R)$ and $E_f(R)$ which enter the phase of the integrand in (2), and the molecular (or perturbed-atom) wave functions Φ_i and Φ_f. In general, we shall retain the lowest-order approximation of these quantities needed to obtain the distinctive features of the LICET and LICCT cross-section line shapes.

III. LASER-INDUCED COLLISIONAL EXCITATION TRANSFER

In this section we present a detailed application of the theory to the LICET process

$$\mathrm{Sr}(5p\,{}^1P_1)+\mathrm{Li}(2s\,{}^2S_{1/2})+\hbar\omega(670\ \mathrm{nm}) \rightarrow \mathrm{Sr}(5s^2\,{}^1S_0)+\mathrm{Li}(4d\,{}^2D_{5/2}) , \quad (4)$$

which has been studied extensively in the measurements of Zhang, Nikolaus, and Toschek.[10] A partial energy-level diagram is given in Fig. 1.

We first note that since both atoms change state, the dipole matrix element in (2) would vanish for the simple separated-atom product wave functions. It is thus necessary to improve the initial and/or final wave function by the introduction of quasimolecular character which results from the interatomic interaction H_c. The longest-ranged term in H_c for neutral atoms is the dipole-dipole interaction

$$H_{dd}=\frac{1}{R^3}[\mathbf{r}_a\cdot\mathbf{r}_b-3(\hat{\mathbf{R}}\cdot\mathbf{r}_a)(\hat{\mathbf{R}}\cdot\mathbf{r}_b)] , \quad (5)$$

where $\mathbf{r}_{a,b}$ indicate a sum over all active (outer) electrons on each atom. The near-energy-resonance (Fig. 1) between $\mathrm{Sr}(5p\,{}^1P_1)$–$\mathrm{Sr}(5s^2\,{}^1S_0)$ (21 698 cm^{-1}) and $\mathrm{Li}(4d\,{}^2D)$–$\mathrm{Li}(2p\,{}^2P)$ (21 719 cm^{-1}) will lead to a much larger perturbation of $\Phi_f^{(0)}$ than $\Phi_i^{(0)}$ by the dipole-dipole interaction.

Applying first-order stationary-state perturbation theory,

$$\Phi_f^{(1)}=\Phi_f^{(0)}+\sum_{n,l,m} a_{nlm}(\mathbf{R})\Phi_{nlm}^{(0)} , \quad (6)$$

where $\Phi_{nlm}^{(0)}$ is the separated-atom wave function for the $\mathrm{Sr}(5p\,{}^1P_1)+\mathrm{Li}(2p\,{}^2P_J)$ intermediate state. The nlm index refers to these quantum numbers for both atoms. Thus, a_{nlm} will contain the small energy denominator Δ resulting from the above near-resonance, while it also depends on the direction $\hat{\mathbf{R}}$ and is proportional to R^{-3} as indicated in (5). The m sum is to be taken over all the degenerate magnetic quantum numbers associated with both atoms. Since $\mathrm{Sr}(5p\,{}^1P_1)$ occurs in both the intermediate state $\Phi_{nlm}^{(0)}$ and the initial state $\Phi_i^{(0)}$, the dipole matrix ele-

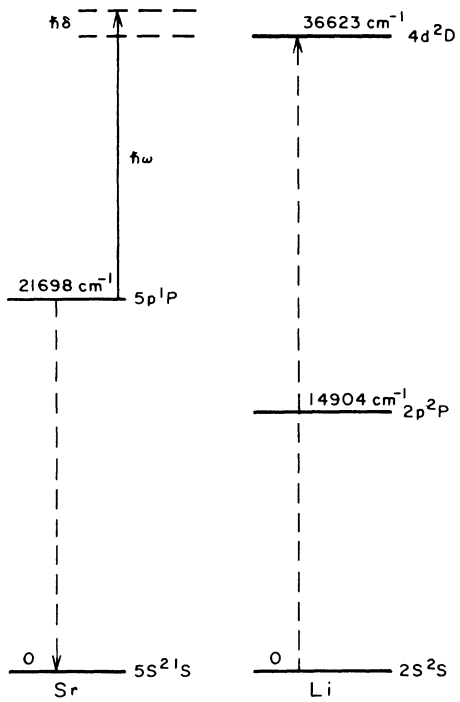

FIG. 1. Partial energy-level diagrams for Sr and Li showing important states for LICET process (4).

ment in (2) no longer vanishes, and has a value proportional to a_{nlm}.

The dipole-dipole interaction (5) may be rewritten in the form

$$H_{\rm dd}=\frac{1}{R^3}\left\{x_a x_b\left[1-3\left[\frac{vt}{R}\right]^2\right]+y_a y_b\left[1-3\left[\frac{\rho}{R}\right]^2\right]-3\frac{\rho vt}{R^2}(x_a y_b+y_a x_b)+z_a z_b\right\}, \quad (7)$$

where the relative velocity is taken along X, the XY plane is the collision plane, and $t=0$ occurs at the distance of closest approach. From this we see that there are three independent trajectory integrals which enter:

$$T_1=\int_0^\infty dt\frac{1}{R^3}\cos[\delta t-\phi(t)]\,,$$
$$T_2=\int_0^\infty dt\frac{(vt)^2}{R^5}\cos[\delta t-\phi(t)]\,, \quad (8)$$
$$T_3=\int_0^\infty dt\frac{\rho vt}{R^5}\sin[\delta t-\phi(t)]\,.$$

The integral occurring in the phase is

$$\phi(t)=\int_0^t dt'\Delta E(R)=\int_0^t dt'\{E_f(R)-E_f(\infty)-[E_i(R)-E_i(\infty)]\}$$

and may be evaluated in closed form for the asymptotic integrand $\Delta C_6/R^6$, where $\Delta C_6=C_6^{(f)}-C_6^{(i)}$. An evaluation of the van der Waals coefficients for this system using Bates-Damgaard atomic radial matrix elements gives

$$C_6^{(i)}=6.63\times10^2 \text{ a.u.}\,,$$
$$C_6^{(f)}=1.30\times10^5 \text{ a.u.}$$

The large magnitude for $C_6^{(f)}$ is also attributable to the same small energy denominator $\Delta=21$ cm^{-1} which makes a_{nlm} large, but we have included many other intermediate states which contribute appreciably to the C_6's.

Averaging over initial and summing over final m states, and averaging over all orientations between laser polarization $\hat{\epsilon}$ and collision plane, we find the following for the transition probability:

$$P(\rho)=\frac{8}{27}\frac{E_0^2}{\Delta^2}(5p\mid r\mid 5s)_{\rm Sr}^2(2s\mid r\mid 2p)_{\rm Li}^2(2p\mid r\mid 4d)_{\rm Li}^2\times(\tfrac{24}{7}T_1^2+T_2^2+T_3^2-T_1T_2)\,. \quad (9)$$

As this is based on first-order perturbation theory it can be expected to be valid only if $P(\rho)\ll1$. Other authors[5,11] solve the two-state coupled equations in $a_{ii}(t)$ and $a_{if}(t)$ to which the time-dependent Schrödinger equation reduces. That procedure is more laborious computationally but ensures that transition probabilities will not violate unitarity. Our expression (9) will certainly give $P(\rho)>1$ for sufficiently high values of laser intensity, and thus cannot be used in every case as it stands. Since a two-state strongly coupled situation gives $P(\rho)$ which would oscillate rapidly as $\sin^2$ between 0 and 1, we model this behavior by letting $P(\rho)=\frac{1}{2}$ for all ρ for which Eq. (9) would lead to a probability exceeding 1. This imposition of unitarity is an approximation which we believe is good to the order of 20%, well within the uncertainties expected from the other approximations made.[12] The trajectory integrals are evaluated numerically. To avoid the problems of doing a quadrature in the region of small R where $\Delta C_6/R^6$ becomes very large, we introduce a cutoff R_0, such that for $R\le R_0$, $\Delta C_6/R^6$ is cut off to the constant value $\Delta C_6/R_0^6$ and $1/R^3$ and (8) is truncated to $1/R_0^3$.

This cutoff in the phase will only be felt for detunings $\delta\sim\Delta C_6/R_0^6$, which are very far out in the quasistatic wing of the line. We use $R_0=20$ which corresponds to $\Delta C_6/R_0^6=222$ cm^{-1}, so our results at appreciably smaller detunings than this value will be essentially unaffected by the cutoff. Another way of seeing that this cutoff will not affect the central part of the line is to note that it is much smaller than the Weisskopf radius 35.3 a.u. The cutoff of $1/R^3$ is consistent with the physical condition that the dipole matrix element of the quasimolecule cannot go as $1/R^3$ to the $R\to0$ limit but rather must approach a finite value representing the united atom. We use the Bates-Damgaard radial matrix elements $(5p\mid r\mid 5s)_{\rm Sr}=3.870$, $(2s\mid r\mid 2p)_{\rm Li}=3.889$, and $(2p\mid r\mid 4d)_{\rm Li}=-1.962$. All present LICET calculations are done for the rms relative velocity $(3kT/M)^{1/2}$ for a temperature of 700 °C.

A comparison of our low-field line shape with the measurement of Zhang, Nikolaus, and Toschek[10] is given in Fig. 2. The absolute measurement of a peak cross section of 2×10^{-13} cm^2 at 1 MW/cm^2 light flux compares very well with our calculated value of 2.23×10^{-13} cm^2. Also the quasistatic wing ($\delta>0$) of both the measurement and calculation vary as $\delta^{-1/2}$, which is consistent with the quasistatic theory discussed below.

In the limit where the atomic motion is negligible in the effective time for photon absorption, and we are not at stationary points of the difference potential, these processes may be regarded as governed by the quasistatic law

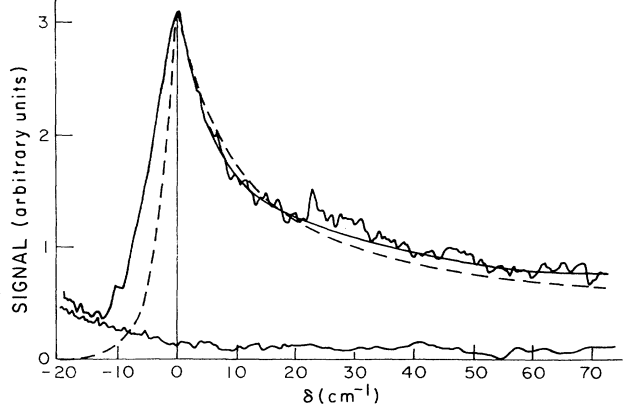

FIG. 2. Low-field cross-section line shape for LICET process (4). Calculation is dashed line. Measurement is that of Zhang *et al.* (Ref. 10) for the fluorescence signal for the process (including background signal). The smooth solid line through the measured signal indicates the behavior of $\delta^{-1/2}$ for $\delta>5$ cm^{-1}.

$$\sigma(\delta)\sim R^2|\mu(R)|^2\Big/\left|\frac{d\Delta E(R)}{dR}\right|, \tag{10}$$

where the energy resonance condition requires that the photon is absorbed at a given R such that $\delta=\Delta E(R)$. This has previously been used successfully in the far quasistatic wing in the atomic line broadening problem, where if $\Delta E=\Delta C_6/R^6$, and $\mu(R)$ is a constant, $R\sim\delta^{-1/6}$ and $\sigma\sim\delta^{-3/2}$.

In the present LICET problem, $\mu(R)\sim 1/R^3$ and $\sigma\sim\delta^{-1/2}$ in the far quasistatic wing, which agrees with both the measurement and present calculation as shown in Fig. 2. Of course this quasistatic behavior does not apply in the core of the line, where σ goes to a finite value as $\delta\to 0$, nor can it apply to any of the antistatic wing where $\delta<0$ (assuming $\Delta C_6>0$). In these regions one must use the full dynamic theory as given here or some suitable variant of it. The full dynamic theory clearly contains a velocity dependence which is not present in (10) and a more complicated dependence upon $\mu(R)$ and $\Delta E(R)$.

In Fig. 3 we show transition probabilities as a function of impact parameter for zero detuning at three laser intensities. For the lowest intensity (10^5 W/cm^2) there are no saturation effects. For a factor of 10 higher intensity one sees how calculated probabilities which exceed one are clipped down to the average value of $\frac{1}{2}$ in accordance with the unitarization approximation we have discussed above. This trend continues for higher intensities where for practically all $\rho<\rho_c$ the average probability of $\frac{1}{2}$ prevails, where ρ_c is the largest value of ρ for which $P(\rho)=1$. For $\rho>\rho_c$ the probability decreases as $1/v^2\rho^4$ (for $\delta=0$ only). For $\delta\neq 0$ the limiting form of $P(\rho)$ is $(\delta^2/v^4\rho^2)K_1^2(\rho\delta/v)$. This dependence arises from the fact that

$$T_1 \underset{\rho\to\infty}{\sim} (\delta/v^2\rho)K_1(\rho\delta/v)$$

and the other T_n's have similar limiting forms.

Figure 4 indicates how the line shape becomes symmetrical as the laser intensity increases. Most of the change in shape occurs on the quasistatic wing ($\delta>0$) but for high enough intensities changes also occur on the antistatic wing ($\delta<0$). The general trend of the line shape becoming more symmetric with decreasing full width at half maximum (FWHM) as the intensity increases agrees with the conclusions of Payne, Anderson, and Turner[5] (see their Fig. 8), Lisitsa and Yakovlenko[3] and Harris and White.[11] Because of the need to solve a transcendental equation to obtain ρ_c, and the cross section being given by $\sigma\cong(\pi/2)\rho_c^2+2\pi\int_{\rho_c}^{\infty}d\rho\,\rho P$, it does not appear that any simple analytic form can be given for the high-intensity line shape. However, the qualitative form of the line shape at high intensities appears to contain the far-wing behavior $|\delta|^{-1}$, with peak value $\sim I^{1/2}$ and FWHM approximately $I^{-1/4}$.

In Fig. 5 we show the approach to symmetric line shapes by graphing a few σ's at fixed detuning as a function of intensity. We note that at low intensities all $\sigma(\delta)$ are linear in I while highly asymmetric. All $\sigma(\delta)$ will bend over due to the saturation effects and end up with the limiting intensity dependence $I^{\nu(|\delta|)}$, where $\nu(0)=\frac{1}{2}$ and $\nu(|\delta|)$ is a decreasing function of $|\delta|$. We find, in the present case, ν (5 cm^{-1})$=0.245$ and ν(10 cm^{-1}) $=0.200$. It is clear that the high-intensity line shape must be symmetric in δ since T_1^2, T_2^2, T_3^2, and T_1T_2, which determine ρ_c, are independent of the sign of δ in the large-ρ limit. Note that the $I^{1/2}$ form of $\sigma(0)$ is a limiting behavior, and any measurement of the maximum

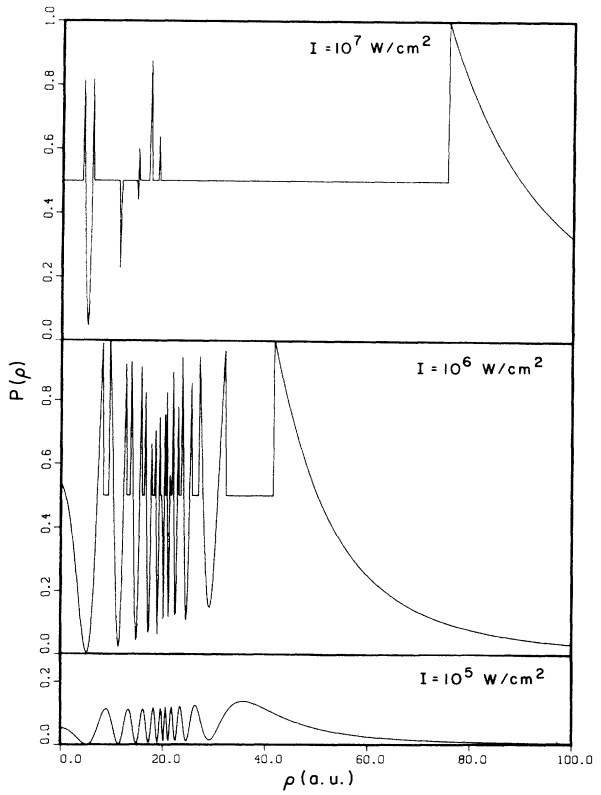

FIG. 3. Typical transition probabilities for LICET process (4) as a function of impact parameter for zero detuning and various laser intensities.

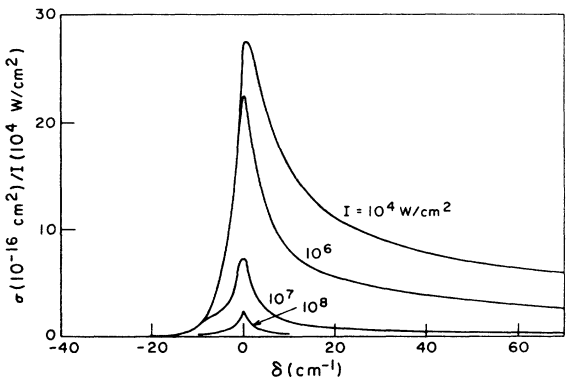

FIG. 4. Calculated line shapes for LICET process (4) for various laser intensities. The line shape does not change for $I<10^4$ W/cm^2.

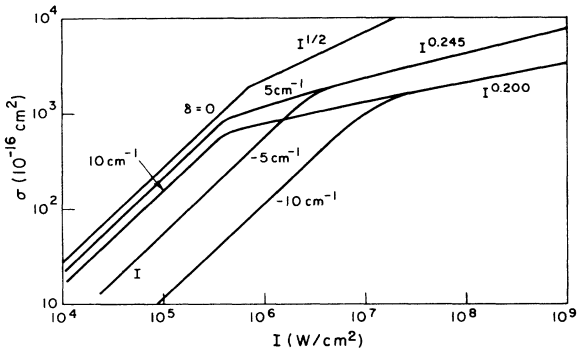

FIG. 5. Calculated intensity dependence for various detunings of the LICET cross section for process (4). The powers of I indicate intensity dependences.

cross section with a finite spectral resolution will necessarily give a result which will move below the $I^{1/2}$ dependence at some high intensity.

IV. LASER-INDUCED COLLISIONAL CHARGE TRANSFER

We now apply the above theory to the LICCT case, and in particular to the process

$$\mathrm{Ca}^+(4s\,^2S_{1/2})+\mathrm{Sr}(5s^2\,^1S_0)+\hbar\omega \rightarrow \mathrm{Ca}(4s^2\,^1S_0)+\mathrm{Sr}^+(5p\,^2P_J)\ , \quad (11)$$

where the asymptotic energy difference corresponds to photon wavelengths of 473 nm for $J=\frac{3}{2}$ and 492 nm for $J=\frac{1}{2}$ (see Fig. 6). The measurements of the cross sections for these processes were carried out by Wright *et al.*,[8] and their results show striking qualitative differences from the line shapes seen in the LICET process as discussed in Sec. III. They found very large positive energy shifts of the LICCT lines from the asymptotic energy differences, and the lines themselves were almost symmetric, even for low laser intensities.

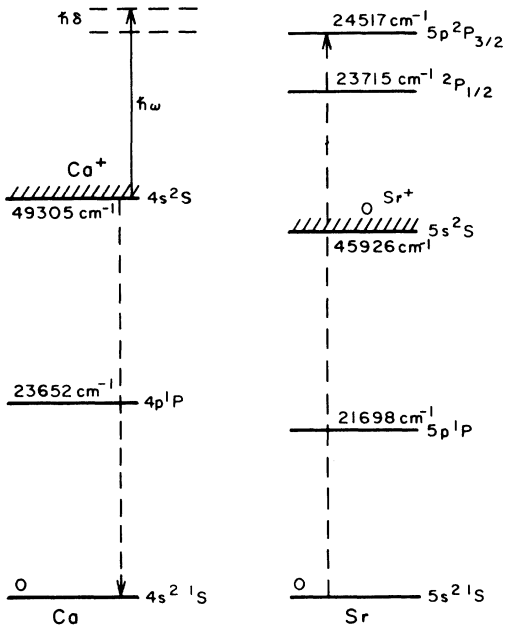

FIG. 6. Partial energy-level diagrams for Ca, Ca$^+$, Sr, and Sr$^+$ showing the important states for LICCT process (11).

In applying the present theory we start with Eq. (2), and note that $E_{i,f}$ must now also contain a polarizability term, $-\alpha/2R^4$. Furthermore, there is a nonvanishing value for the dipole matrix element even in the separated-atom forms for $\Phi_{i,f}$. These states are the three-electron wave functions

$$\Phi_i^{(0)}=|\,\mathrm{Ca}^+(4s\,^2S_{1/2})\rangle\,|\,\mathrm{Sr}(5s^2\,^1S_0)\rangle\ ,$$
$$\Phi_f^{(0)}=|\,\mathrm{Ca}(4s^2\,^1S_0)\rangle\,|\,\mathrm{Sr}^+(5p\,^2P_J)\rangle\ . \quad (12)$$

From this it can be seen that there is a nonvanishing dipole matrix element between $\mathrm{Sr}^+(5p\,^2P_J)$ and one of the $5s$ electrons in $\mathrm{Sr}(5s^2\,^1S_0)$. This matrix element is multiplied by an overlap integral between $\mathrm{Ca}^+(4s\,^2S_{1/2})$ and one of the $4s$ electrons in $\mathrm{Ca}(4s^2\,^1S_0)$, and also by an overlap integral of the other $4s$ electron in $\mathrm{Ca}(4s^2\,^1S_0)$ and the second $5s$ electron in $\mathrm{Sr}(5s^2\,^1S_0)$. Since this latter overlap integral involves an electron which is transferred from one atomic center to the other, it will be a short-ranged function of R.

Carrying out the appropriate angular algebra for the two possible final fine-structure states $J=\frac{1}{2}$ and $\frac{3}{2}$, we find the transition probability to be

$$P_J(\rho)=\frac{E_0^2}{72}(2J+1)(\mathrm{Ca}(4s)\,|\,\mathrm{Ca}^+(4s))^2 \times(\mathrm{Sr}(5s)\,|\,r\,|\,\mathrm{Sr}^+(5p))^2T_J^2\ , \quad (13)$$

where the trajectory integral is

$$T_J=\int_0^\infty dt\,F(R)\cos[\delta t-\phi_J(t)]\ . \quad (14)$$

Here $F(R)$ is the two-center overlap integral $\langle \mathrm{Ca}(4s)\,|\,\mathrm{Sr}(5s)\rangle$, which depends only on the magnitude of R since we are dealing with s orbitals. We use Bates-Damgaard wave functions, which give the radial matrix elements $(\mathrm{Ca}(4s)\,|\,\mathrm{Ca}^+(4s))=0.926$ and $(\mathrm{Sr}(5s)\,|\,r\,|\,\mathrm{Sr}^+(5p))=-3.885$, and find the $F(R)$ given in Fig. 7. We use the recommended values[13] for atomic polarizabilities

$$\alpha_i=\alpha(\mathrm{Sr}(5s^2\,^1S_0))=168.6\ \text{a.u.}$$

and

$$\alpha_f=\alpha(\mathrm{Ca}(4s^2\,^1S_0))=186.0\ \text{a.u.}\ ,$$

and evaluate the following van der Waals coefficients with the use of Bates-Damgaard radial matrix elements:

$$C_6^{(i)}=-2.21\times10^3\ \text{a.u.}\ ,$$
$$C_6^{(f)}(J=\tfrac{1}{2})=5.59\times10^5\ \text{a.u.}\ ,$$
$$C_6^{(f)}(J=\tfrac{3}{2})=3.61\times10^4\ \text{a.u.}$$

The large difference in $C_6^{(f)}$'s for the two fine-structure

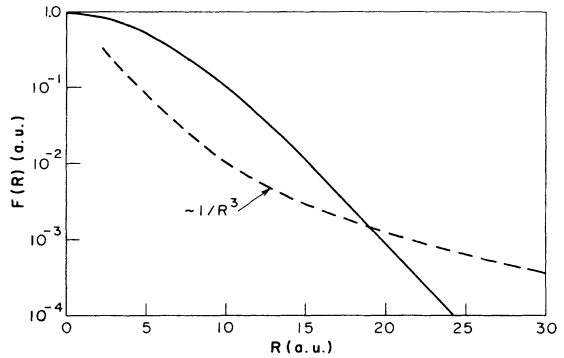

FIG. 7. The transition matrix element $F(R) = \langle \mathrm{Ca}(4s) \mid \mathrm{Sr}(5s) \rangle$ for the LICCT process (11). It has the asymptotic form $15.5\, e^{-0.491R}$. Also shown for comparison is a curve proportional to $1/R^3$, the variation of the effective transition matrix element for the LICET process.

components of the final-state Sr^+ ion arises because the fine-structure splittings in intermediate states are large enough to affect the energy denominators significantly. The asymptotic potential curves and the difference curves are shown in Fig. 8. Note that the diabatic curves for $E_f(J=\frac{3}{2})$ and $E_f(J=\frac{1}{2})$ cross at $R \cong 23$ a.u. Since $\Delta\alpha$ is small and $\Delta C_6^{(J)}$ is large and positive for both J values, one expects at least a large asymmetry of $\sigma_J(\delta)$ toward $\delta > 0$. The main qualitative difference between the

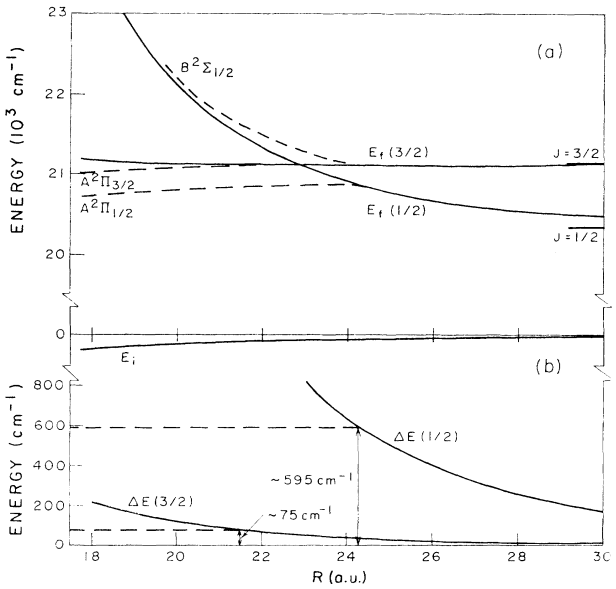

FIG. 8. (a) Asymptotic potential curves and (b) difference potential curves, $\Delta E = E_f(R) - E_f(\infty) - [E_i(R) - E_i(\infty)]$, for LICCT process (11). The solid lines are the diabatic curves based upon the polarization and van der Waals interactions for the initial and final states. The dashed extensions of the difference potentials are the cutoffs used to fit the LICCT shift data. They correspond to the dashed extensions for the $A\,^2\Pi_{1/2,3/2}$ final-state adiabatic curves. The dashed line in the $B\,^2\Sigma_{1/2}$ curve is purely schematic.

LICCT (13) and LICET probabilities (9) is the occurrence of an exponentially decreasing $F(R)$ compared with a $1/R^3$ factor in their respective trajectory integrals.

In attempting to apply the quasistatic law (10) to the LICCT process, one can identify the effective molecular dipole matrix element $\mu(R)$ as proportional to the overlap coefficient $F(R)$ occurring in (14). If we ignore for now the small contribution of the polarization interaction (since $\Delta\alpha$ is so small in the particular case we are studying), then again $\Delta E \simeq \Delta C_6/R^6$, and taking $F \sim \exp(-\beta R)$, we find from (10) that

$$\sigma \sim \delta^{-3/2} \exp[-2\beta(\Delta C_6/\delta)^{1/6}] \,. \tag{15}$$

Unlike the atomic line broadening and LICET cases, which were consistent with a line centered at $\delta = 0$, this is consistent with a cross section having its maximum value shifted to some positive value of δ. This is apparent because $\delta^{-3/2}$ is monotonically decreasing and $\exp[-2\beta(\Delta C_6/\delta)^{1/6}]$ is a monotonically increasing function of δ.

However, the result of applying the above quasistatic formula directly to the present LICCT problem leads to very bad results if no cutoffs or modifications are applied to the asymptotic potentials. One finds shifts of the order of 50 000 cm^{-1} for $J=\frac{1}{2}$ and 10 000 cm^{-1} for $J=\frac{3}{2}$, and FWHM's of the same order of magnitude, very different from the values of 595 and 75 cm^{-1}, respectively, found in the measurement. Both of these quasistatic maxima correspond to R of about 10 a.u., which is a region of questionable validity for the asymptotic difference potential being used.

This indicates that, unlike in the LICET case, the choice of a cutoff or modification of the asymptotic potentials is crucial in the determination of the details of the shifted LICCT profile. As a first step we again take the simple cutoff $\Delta E_J(R) = \Delta E_J(R_0)$ for $R < R_0$, and adjust R_0 for each J so that the LICCT cross section is centered at the observed detuning. This leads to the condition that $\Delta E_J(R_0)$ is just equal to observed detuning δ_0, as would be expected from the quasistatic law (10). However, we cannot use that form for a detailed description of the line shape since the $d\Delta E/dR$ in the denominator vanishes over the entire region $R=0$ to R_0 in our model. The dynamic theory yields the approximate trajectory integral for (14),

$$\begin{aligned} T &\sim \int_0^\infty dt\, e^{-\beta R} \cos[(\delta-\delta_0)t] \\ &= \frac{\rho\beta}{v} \left[\left[\frac{\delta-\delta_0}{v} \right]^2 + \beta^2 \right]^{-1/2} \\ &\quad \times K_1 \left\{ \rho \left[\left[\frac{\delta-\delta_0}{v} \right]^2 + \beta^2 \right]^{1/2} \right\}, \end{aligned} \tag{16}$$

where we have approximated $F(R)$ by $ce^{-\beta R}$. Note that because of the exponential decay of $F(R)$, the part of the integral from $t = (1/v)(R_0^2 - \rho^2)^{1/2}$ to ∞ is negligible. This indicates that the basic line shape is a Lorentzian, which is modulated by the Bessel-function coefficients. It also leads to the central cross section varying as $I/v^2\beta^4$, and being approximately the same for both J's.

From the measured shifts of $\delta_0(J=\frac{1}{2})=595$ cm^{-1} and $\delta_0(J=\frac{3}{2})=75$ cm^{-1} and our asymptotically calculated potentials, we find the cutoffs $R_0(J=\frac{1}{2})=24.28$ a.u. and $R_0(J=\frac{3}{2})=21.50$ a.u. Thus, the larger shift is correlated with the larger calculated $C_6^{(f)}$ coefficient, and we also note that the fitted R_0's lie on either side of the crossing point (23 a.u.) of the diabatic final-state potential curves. This is consistent with the fact that the adiabatic molecular curves for this system would not cross but rather repel one another in this region. The asymptotic $J=\frac{1}{2}$ diabatic curve goes into an adiabatic $A\,^2\Pi_{1/2}$ curve, and the $J=\frac{3}{2}$ diabatic curve splits into $A\,^2\Pi_{3/2}$ and $B\,^2\Sigma_{1/2}$ adiabatic curves (see, for example, Ref. 14).

The effect of our cutoff of the difference potential curves is equivalent to the modification of the E_f curves indicated in Fig. 8 (assuming that E_i remains unchanged). Since the uppermost $B\,^2\Sigma_{1/2}$ curve rises sharply we do not identify it with either of the two observed LICCT peaks, but rather associate them with the lower-lying $A\,^2\Pi_{1/2}$ and $A\,^2\Pi_{3/2}$ curves. Since it is unlikely that the $B\,^2\Sigma_{1/2}$ curve will have a stationary point at moderate R, there is probably no LICCT peak associated with it. However, we must remove its statistical weight from our Eq. (13), and recognize that each of the $A\,^2\Pi$ states have an equal statistical weight of 2, by replacing $(2J+1)$ in (13) by the factor 2 (for both J's). The use of the cutoff difference potentials is now consistent with the adiabatic $A\,^2\Pi$ curves given in Fig. 8, and the empirical magnitudes for the R_0's are consistent with the avoided crossing of the calculated diabatic curves.

We have not made any short-range modifications in $F(R)$ since it is well behaved into $R\rightarrow 0$. Since the present LICCT cross sections strongly depend on contributions to the trajectory integrals at small R, and in reality the two atoms have strong repulsive forces at small separations, we have introduced a hard-sphere radius $R_{\rm HS}$ as an additional parameter. The trajectory is assumed to undergo specular reflection at $R_{\rm HS}$ when $\rho<R_{\rm HS}$. The effect of this is to exclude a region where $F(R)$ is its largest, and thus reduce the magnitudes of the LICCT cross sections. We have chosen $R_{\rm HS}=9$ a.u. as a value which is reasonable on the basis of known atom-atom low-energy scattering measurements[15] and *ab initio* theory for other cases,[14] as well as for providing a reasonable fit to the absolute LICCT cross sections measured by Wright *et al.*[8] We apply the same unitarization procedure as before, but it does not come into play until much higher laser powers because the present LICCT transition probabilities are much smaller than those of the LICET case studied. All calculations for the LICCT process are done for the rms relative velocity at a temperature of 850°C (used in the measurement).

The resulting LICCT cross sections are compared in Fig. 9 with the observed fluorescence signals which are the signature of the process in the experiment.[8] The calculated LICCT line shapes are quite symmetric and have FWHM's which are about $\frac{1}{3}$ of the observed widths (apart from the additional broad feature in the $J=\frac{1}{2}$ measured spectrum). The calculated widths could be expected to increase with some softening of the sharp cutoff which we are using, and with more curvature in the trajectories, as is present in the real situation.

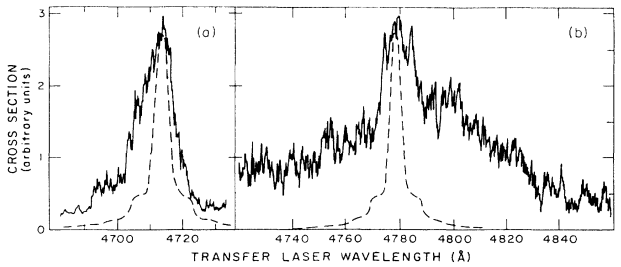

FIG. 9. Comparison of calculated low-intensity wavelength variation of LICCT cross sections for process (11): (a) for $J=\frac{1}{2}$, (b) for $J=\frac{3}{2}$ (dashed lines), with experimental traces of fluorescence signals for these processes (Ref. 8).

A graph of the calculated LICCT transition probability as a function of impact parameter is given for $J=\frac{3}{2}$ in Fig. 10 for two laser intensities. The effect of the exclusion of the trajectory from the inner hard sphere is to scoop out transition probability for $\rho<R_{\rm HS}$. The unsaturated $P(\rho)$ does not have the oscillations found in the LICET case, which indicates that $\phi(\infty)$ does not now have as much variation with ρ as in the LICET calculation (see Robinson, Ref. 3). The introduction of some rounding in ΔE for $R<R_0$ is seen to restore these oscillations. The imposition of our unitarization procedure at the higher intensity in Fig. 10 produces the intermediate region of $P=\frac{1}{2}$. This onset of saturation in the LICCT transition probability, as in the LICET case, leads to a departure of the cross section from its linear variation with laser intensity.

The variation in cross-section line shape with intensity is shown in Fig. 11. These are rather unusual looking line shapes, but it is intriguing to note that the measured profiles in Fig. 9 also appear to have shoulder or pedestal structure. The increasing widths with increasing intensity

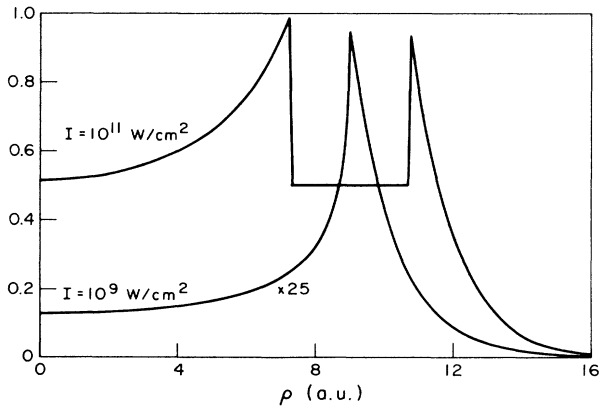

FIG. 10. Transition probabilities for LICCT process (11) for $J=\frac{3}{2}$ and at the detuning for maximum cross section, $\delta_0=75$ cm^{-1}, for two laser intensities. The $J=\frac{1}{2}$ results at its maximum, $\delta_0=595$ cm^{-1}, are very similar.

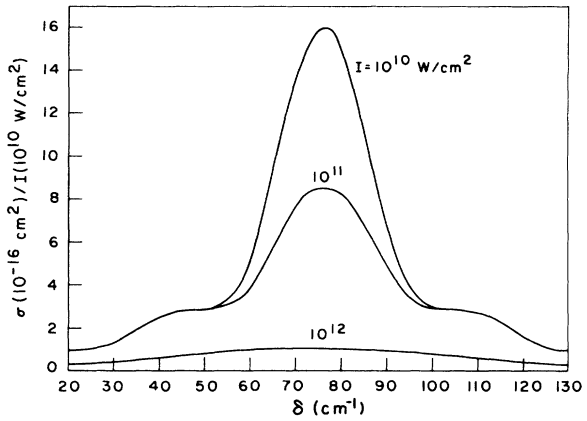

FIG. 11. Calculated cross-section line shapes for the LICCT process (11) for $J=\frac{3}{2}$ for various laser intensities. The $J=\frac{1}{2}$ results centered at $\delta_0=595$ cm^{-1} are very similar.

is in sharp contrast to the decreasing widths occurring for LICET (see Fig. 4). This behavior can be understood to arise from the exponential decrease of $F(R)$, the overlap integral which is the effective transition matrix element for the LICCT process. As an extreme case of short-range behavior consider the sharp cutoff where $F(R)=0$ for $R>R_c$. Then it is clear that $P(\rho)=0$ for $\rho>R_c$, and at moderate intensities a line shape is present because $P(\rho)$ for $\rho\leq R_c$ will maximize around some central value of detuning. However, as the intensity increases $P(\rho)$ will increase until it saturates at $\frac{1}{2}$. The effect of limiting the growth of $P(\rho)$ by both the unitary condition and the cutoff at $\rho=R_c$ is to produce a cross section which cannot exceed $(\pi/2)R_c^2$, and this limit holds for all detunings. The result is a line width which increases indefinitely with I, since the central value is bounded and the wings continue to increase toward this bound.

Figure 12 contains the calculated LICCT cross sections

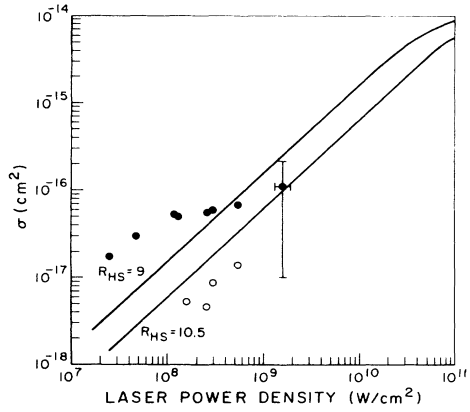

FIG. 12. Maximum cross section for the LICCT process (11) as a function of laser intensity. Presently calculated (solid lines) and measured values of Ref. 8 (solid circles $J=\frac{3}{2}$, open circles $J=\frac{1}{2}$). The typical experimental error bar shown applies to each of the measured points.

(at their tuned maximum value) as a function of laser intensity. At line center our present model gives a negligible difference in LICCT cross section for the two final fine-structure states. This follows from the effective J independence of the trajectory integral (16) at $\delta=\delta_0$ and the equal statistical weights for the adiabatic molecular states. A more precise description of the inner behavior of these adiabatic difference potential curves would very likely lead to different maximum cross sections. For example, if a localized maximum occurred in ΔE near R_0, a large contribution to the trajectory integral would come from the region of the maximum since it is a stationary phase point. This should lead to $\sigma(J=\frac{3}{2})>\sigma(J=\frac{1}{2})$ because $R_0(J=\frac{3}{2})<R_0(J=\frac{1}{2})$, and $F^2[R_0(J=\frac{3}{2})]>F^2[R_0(J=\frac{1}{2})]$, which is consistent with the measurement. With our choice of $R_{HS}=9$ the calculated cross sections are essentially within all the error bars associated with the $J=\frac{3}{2}$ measured points. This puts them about a factor of 2 above the upper edge of the error bars associated with the $J=\frac{1}{2}$ measured points. This factor of 2 could easily be accounted for by the use of a better difference potential, as discussed above.

A more serious potential discrepancy lies in the apparent nonlinearity of the $J=\frac{3}{2}$ data points. We are unable to suggest any theoretical modification which would give a departure from linearity at an intensity as low as 10^8 W/cm^2, where the $J=\frac{3}{2}$ data appear to have a change in slope. Our calculations begin to show saturation effects only at $I\gtrsim 10^{10}$ W/cm^2. However, the error bars correspond to an uncertainty in absolute cross section of about a factor 20 *at each intensity.* Since each point corresponds to a completely independent measurement[16] the full error bar must be allowed for each of the points, and this then *does not exclude* linear behavior over the range of the $J=\frac{3}{2}$ measured points. In fact, our calculated curve is at the top of a band of straight lines linear in the intensity and covering about a factor of 3 in magnitude, which would run through all the error bars of the $J=\frac{3}{2}$ points. The line at the bottom of this band would be consistent with most of the data points (both $J=\frac{1}{2}$ and $\frac{3}{2}$, excepting the one low $J=\frac{1}{2}$ point), but would require a hard-sphere radius in our model of about 10.5 a.u., which is probably somewhat unrealistically too large.

V. SUMMARY

We have outlined the standard theory for describing laser-induced collision processes, and have applied it to particular LICET and LICCT transitions which have been experimentally studied in considerable detail. Additional approximations have been made in cutting off the phase interaction energies, in altering trajectories in a reasonable way at small interatomic separations, and in unitarizing transition probabilities at high laser intensities. The characteristic low-intensity asymmetry of the LICET process is well represented in the calculation, and the peak cross section is obtained within 25% of the experimental estimate. The asymmetry of the LICET line shape is seen to disappear as laser intensity is increased and the linewidths are seen to decrease, in agreement with previ-

ous theoretical work.

The treatment of the LICCT process by a similar theory shows that the dipole-dipole transition matrix element of the LICET process is replaced by an overlap integral of much shorter range. This has the effect of introducing large shifts in the laser wavelength for maximum cross section as well as drastically reducing the magnitude of the cross section from the calculated LICET values. The observed shifts in the measurements of Wright *et al.*[8] can be fitted by a simple difference potential model which is consistent with an interpretation in terms of adiabatic potential curves. The measured cross-section magnitudes can be obtained with the use of a reasonable hard-sphere radius in the calculation. The expected linear dependence of cross section with laser intensity is not inconsistent with the measurements, but the agreement is not entirely satisfactory. At higher intensities, when saturation sets in, the calculated maximum cross sections increase more slowly than linearly with laser intensity. The LICCT cross section widths also increase with intensity (unlike the LICET case).

ACKNOWLEDGMENTS

I would like to thank Peter Toschek, Alan Gallagher, Jean Pascale, John Delos, Michael Wright, and Stephen Harris for very helpful discussions, and Chela Kunasz and Steve ONeil for computing advice. This work was partially supported by the National Science Foundation through Grant No. PHY86-04504, and all computations were done on the Joint Institute for Laboratory Astrophysics (JILA) VAX 8600.

---

[1]L. I. Gudzenko and S. I. Yakovlenko, Zh. Eksp. Teor. Fiz. **62**, 1686 (1972) [Sov. Phys.—JETP **35**, 877 (1972)].

[2]A. Gallagher and T. Holstein, Phys. Rev. A **16**, 2413 (1977).

[3]V. S. Lisitsa and S. I. Yakovlenko, Zh. Eksp. Teor. Fiz. **66**, 1550 (1974) [Sov. Phys.—JETP **39**, 759 (1974)]; S. Geltman, J. Phys. B **9**, L569 (1976); A. M. F. Lau, Phys. Rev. A **14**, 279 (1976); P. L. Knight, J. Phys. B **10**, L195 (1977); J.-M. Yuan, J. R. Laing, and T. F. George, J. Chem. Phys. **66**, 1107 (1977); M. H. Nayfeh and M. G. Payne, Phys. Rev. A **17**, 169 (1978); E. J. Robinson, J. Phys. B **9**, 1451 (1979).

[4]P. R. Berman and E. J. Robinson, in *Photon-Assisted Collisions and Related Topics*, edited by N. K. Rahman and C. Guidotti (Harwood, Chur, 1982), p. 15; R. S. Berry, in *Physics of Electronic and Atomic Collisions*, edited by S. Datz (North-Holland, Amsterdam, 1982), p. 413; F. Roussel, Comments At. Mol. Phys. **15**, 59 (1984); J. Weiner, *ibid.* **16**, 89 (1985).

[5]M. G. Payne, V. E. Anderson, and J. E. Turner, Phys. Rev. A **20**, 1032 (1979).

[6]S. E. Harris and D. B. Lidow, Phys. Rev. Lett. **33**, 674 (1974); R. W. Falcone, W. R. Green, J. C. White, J. F. Young, and S. E. Harris, Phys. Rev. A **15**, 1333 (1977); D. B. Lidow, R. W. Falcone, J. F. Young, and S. E. Harris, Phys. Rev. Lett. **36**, 462 (1976) [**37**, 1590(E) (1976)]; S. E. Harris, R. W. Falcone, W. R. Green, D. B. Lidow, J. C. White, and J. F. Young, in *Tunable Lasers and Applications*, edited by A. Mooradian, T. Jaeger, and P. Stokseth (Springer-Verlag, New York, 1976), p. 193; L. J. Lynch, J. Lukasik, J. F. Young, and S. E. Harris, Phys. Rev. Lett. **40**, 1493 (1978).

[7]Ph. Cahuzac and P. E. Toschek, Phys. Rev. Lett. **40**, 1087 (1978), C. Brechignac, Ph. Cahuzac, and P. E. Toschek, Phys. Rev. A **21**, 1969 (1980).

[8]M. D. Wright, E. L. Ginzton Laboratory Report No. 3330, 1981 (unpublished); W. R. Green, M. D. Wright, J. F. Young, and S. E. Harris, Phys. Rev. Lett. **43**, 120 (1979). [After this manuscript was submitted, another measurement of an LICCT process was published by A. Débarre and Ph. Cahuzac, J. Phys. B **19**, 3965 (1986).]

[9]R. Z. Vitlina, A. V. Chaplik, and M. V. Entin, Zh. Eksp. Teor. Fiz. **67**, 1667 (1974) [Sov. Phys.—JETP **40**, 829 (1975)]; D. A. Copeland and C. L. Tang, J. Chem. Phys. **66**, 5126 (1977).

[10]D. Z. Zhang, B. Nikolaus, and P. E. Toschek, J. Appl. Phys. B **28**, 195 (1982).

[11]S. E. Harris and J. C. White, IEEE J. Quantum Electron. **QE-13**, 972 (1977).

[12]An alternate form of unitarization that would perhaps appear less severe would be to take $P=\sin^2(\sqrt{P_1})$ for all ρ, where P_1 is the first-order nonunitary calculated value [Eq. (9)]. We estimate that the two forms should differ by less than 40% in the region of ρ where $P_1 > 1$, and should lead to differences in σ of about 20% or less.

[13]T. Miller and B. Bederson, Adv. At. Mol. Phys. **13**, 1 (1977).

[14]J. Pascale and J. Vandeplanque, J. Chem. Phys. **60**, 2278 (1974).

[15]R. B. Bernstein and J. T. Muckerman, Adv. Chem. Phys. **12**, 289 (1967).

[16]M. D. Wright (private communication).